MeMeA 2008 – IEEE International
Workshop on Medical Measurements and Applications
Ottawa, Ontario, Canada - May 9-10, 2008

Detection of unreliable measurements in multi-sensor devices

Yednek Asfaw[1], Andy Adler[2]
yasfaw@site.uottawa.ca[1], adler@sce.carleton.ca[2]
[1]School of Information Technology and Engineering (SITE), University Of Ottawa, Canada
[2]Systems and Computer Engineering (SCE), Carleton University, Ottawa, Canada

Abstract *– Multi-sensor monitoring devices that use skin surface or implanted sensors are susceptible to changes in temperature, sweat, and movement, such that the measured data cannot be used. This paper presents an automatic approach to detect such erroneous sensors. It is based on the assumption that valid measurements are related by a reconstruction model, while measurements from erroneous sensors are unrelated. The method estimates the data at each sensor based on the measurements from all other sensors, and compares it to the measurements. The sensor-data match is tested using ANOVA to detect the presence of an erroneous sensor. The method was tested on simulated and experimental data of Electrical Impedance Tomography (EIT) and ECG data which showed consistent identification of erroneous electrodes.*

Keywords *– errors, sensors, reconstruction algorithms*

I. INTRODUCTION

Health care systems worldwide are under pressure to deliver a better and more efficient service. One approach to help deliver such services is technology to enable home and mobile care; several studies have shown that such care improves the patient's quality of life and outcomes, while reducing cost [14, 15]. A key technological component required to enable such care is non-invasive portable biomedical monitoring devices. Such technology enables continuous measurement of parameters as heart and lung activity, blood chemical concentrations, and blood pressure levels. While a growing market provides great incentive for the researchers and companies in the field, there are difficult challenges associated with design of these devices. The monitoring devices typically use skin surface or implanted sensors to measure the electrical and optical properties of the body. These sensors are susceptible to changes in temperature, sweat, and movement with exercise and breathing. For example, it has been shown that electrodes on the body surface give false readings due to electronic interference [4], patient movement, or sweat and peripheral edema [6], especially in long term monitoring applications [5].

For reliable monitoring of patients, it is thus important to detect sensor errors. Unfortunately, it appears that strategies to detect such errors are rarely published and most strategies are largely heuristic measures to verify the goodness of data. One common approach is detection based on identification of unusually large changes in the measurements. The disadvantage is the difficulty of defining an appropriate threshold for unusual measurements that can be applied across different devices.

In this work, we address this issue by proposing an algorithmic framework for detection of unreliable measurements and erroneous sensors in multi-sensor devices for biomedical instrumentation. This paper develops an approach based on explicitly modeling the sensor and device characteristics and using the interrelationships to ascertain the goodness of measurements.

II. METHODS – ALGORITHM

This paper extends the method developed in [1, 2] for electrical impedance tomography (EIT) systems to calculate a measure of sensor reliability for general multi-sensor systems with and without known system model. It identifies sensors subject to data errors or variability, and calculates a measure of the reliability of each sensor's data. Essentially, the algorithm works by inversing the detection criterion: rather than looking for errors, the approach looks for good data, defined by its consistency with other sensor measurements and prior models of sensor behavior.

A. System Model

We assume that the system model of a multi-sensor device may be linearized around an operating point, and expressed as:

$$\mathbf{z} = \mathbf{H}\mathbf{x} \tag{1}$$

where **H** is the linearized observation of model, **z** is a vector representation of measurements from all sensors, and **x** is the vector of system model parameters. **H** is also known as a Jacobean or Sensitivity matrix where it is expressed as a partial derivative of **z** with respect to **x**.

$$\mathbf{H} = \begin{bmatrix} \frac{\partial z_1}{\partial x_1} & \cdots & \frac{\partial z_1}{\partial x_m} \\ \vdots & \ddots & \vdots \\ \frac{\partial z_m}{\partial x_1} & \cdots & \frac{\partial z_m}{\partial x_m} \end{bmatrix} \tag{2}$$

Based on the system model, we calculate a reconstruction model (inverse of the system model) expressed as:

$$\hat{\mathbf{x}} = \mathbf{R}\mathbf{z} \tag{3}$$

where **R** the reconstruction model, and $\hat{\mathbf{x}}$ is the estimate of the system model.

The reconstruction model (**R**) is determined by inverting the system model equation. If the system model fulfills Hadamard condition [6], then **R** can be determined through direct inversion. Otherwise, **R** can be determined using a regularization scheme, such as that of [1]. In a multi-sensor device the characteristics of the system model could either be known or unknown, hence requiring different approaches of determining the observation and reconstruction model.

If the system model is known the underlying principle that defines **H** and **R** is pre-determined. [1] shows an example of a known system model in Electrical Impedance Tomography (EIT). EIT is an imaging technique which calculates the electrical conductivity distribution within a medium from electrical measurements made at a series of electrodes on the medium surface. The observation model (equation 4) defined through a generalized relationship between the background conductivity (**x**) of the medium and the measurements at the boundary (**z**) and is therefore considered to be known.

$$\mathbf{H}_{i,j} = \left.\frac{\partial \mathbf{z}_i}{\partial \mathbf{x}_j}\right|_{\sigma_b=\sigma_0} \tag{4}$$

x is the difference in conductivity of the medium:

$$\mathbf{x} = \sigma^1 - \sigma^2 \tag{5}$$

and **z** is the normalized difference in the voltage measurements $\mathbf{v_i^1}$ and $\mathbf{v_i^2}$ which represents the i^{th} voltage measurements at time t^1 and t^2, respectively:

$$\mathbf{z} = \mathrm{v}_i^1 - \mathrm{v}_i^2 \tag{6}$$

Since this system does not fulfill the Hadamard condition [6], **R** is determined through a regularization scheme as shown in [1] to solve equation 2.

If the system model is unknown, **H** and **R** can only be deduced by applying generalized techniques such as Principle Component Analysis (PCA) or Independent Component Analysis (ICA) on the test data [9, 10]. One such example of a multi-sensor system with unknown system model is Electrocardiogram (ECG). The system uses multiple surface electrodes to monitor the heart activity of a patient. The measured values from each sensor are organized as column vectors in the matrix **z**. To enforce non-singularity the matrix is multiplied by its transpose:

$$\mathbf{D}=\mathbf{z}*\mathbf{z}^{\mathrm{T}} \tag{7}$$

Applying SVD to the square matrix **D** provides us the decomposition into eigenvectors and eigenvalues:

$$\mathbf{D}=\mathbf{U}\boldsymbol{\Sigma}\mathbf{V}^{\mathrm{T}} \tag{8}$$

where **V** is the eigenvector and **Σ** is column matrix of the eigenvalue, The top *n* dominant eigenvectors ($\mathrm{v}^1, \mathrm{v}^2, \mathrm{v}^3, \ldots, \mathrm{v}^n$) can be used to simulate an observation model (equation 9). Therefore, the eigenvectors can be used to build the observation model **H**, where each column of **H** represents the eigenvectors.

$$\mathbf{H} = \begin{bmatrix} v_1^1 & v_1^2 & v_1^3 & \ldots & v_1^n \\ v_2^1 & v_2^2 & v_2^3 & \ldots & v_2^n \\ v_3^1 & v_3^2 & v_3^3 & \ldots & v_3^n \\ \vdots & \vdots & \vdots & \vdots & \vdots \\ v_n^1 & v_n^2 & v_n^3 & \ldots & v_n^n \end{bmatrix} \tag{9}$$

The inverse of the system model, **R,** is determined through direct inversion:

$$\mathbf{R}=(\mathbf{H}^{\mathrm{T}}\mathbf{H})^{-1}\mathbf{H}^{\mathrm{T}} \tag{10}$$

B. Estimation Scheme

The estimation scheme is based on the assumption that a set of good sensors produces internally consistent data as discussed in [3]. Such consistency can be verified by estimating the measured data at each sensor in the set, using only measurements on other sensors, and then comparing the estimate to the actual data measured. The general procedure for the algorithm is outlined as follows:

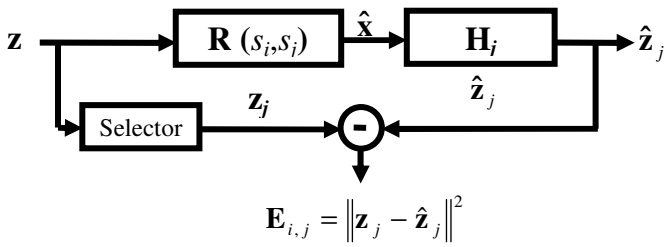

Figure 1: Block Diagram of calculation for estimation error of $\mathbf{E}_j$. $\mathbf{R}(s_i,s_j)$ is the inverse of the system model without the contribution from s_i s_j. Based on the estimate of system model parameters $\hat{\mathbf{x}}$ and $\mathbf{H}_j$, the measurement from sensor s_j can be reconstructed. The difference between the real data and the estimate provides us with an estimation error.

We iterate over each sensor s_i in set *A* (containing all sensors), forming a set *A′* (all sensors not including s_i). In a known system model, the consistency of the data within *A*' is tested by removing s_j and estimating its result based on data from all other remaining sensors. The sum of the estimation error (T_i) from all possible s_j within A' gives an indication of the status of s_i. When an erroneous sensor is removed, the data that remains will be in agreement with the model. If the erroneous sensor is a part of the *A*' set, the estimation error for all sensors within that specific A' set will be high as the erroneous data would not be in agreement with the model.

In devices with unknown system models, the system parameters, **H** and **R,** are estimated for all possible set of sensors by excluding one sensor at a time. In the presence of an erroneous sensor, the noise introduced into the system will dominate all other data coming from all other sensors. Hence, the eigenvectors are good descriptors of the dominant data from the erroneous sensors. Consequentially, a model that excludes the erroneous sensors has a high estimation error

and a model that excludes the non-erroneous sensors results in a low estimation error. Therefore, the consistency test is the sum of estimation error (T_i) for sensor s_i within all possible A'. This approach stems from the fact that **H** and **R** are mainly descriptors of the data and more specifically the dominant noisy data. Therefore, the data fits the model only when the erroneous sensor is part of A'.

In either case, $\mathbf{H}_j$ represents the rows of the sensitivity matrix **H** which correspond to measurements on s_j. $\hat{\mathbf{x}}$ is then calculated from $\hat{\mathbf{x}} = \mathbf{R}(s_i,s_j)\mathbf{z}$, which excludes data from sensors s_i and s_j. The estimate of **z** is determined using equation 1 and the estimation error ($\mathbf{E}_{i,j}$) is determined for all possible sensor pairs s_i and s_j. We have shown that $\mathbf{E}_{i,j}$ can be efficiently calculated in known system models by pre-computing parameters which are independent of data [3].

C. Decision Parameter

If all values of sum of estimation error (T_i) are low, the data set contains all "good" sensors; otherwise it contains at least one erroneous sensor. T_i values are tested against each other to detect if any are significantly less than the others. This is tested using Analysis of Variance (ANOVA) between $\mathbf{E}_i$ of all sensors in set A. For known system model, $\mathbf{E}_i$ represents a list of estimation errors from set A' when sensor s_i is removed. For unknown system model, $\mathbf{E}_i$ represents a list of estimation errors for s_i calculated from all sets A'.

Using the statistical terminology, $\mathbf{E}_i$ are referred to as *Treatments* [8]. ANOVA is used to determine the statistical similarity between the $\mathbf{E}_i$'s by testing the equality of N *Treatment* means ($\mu_1,\mu_2,\mu_3,\ldots,\mu_N$) [8]. The *treatment effect* (τ_i) represents difference of an individual measurement from the overall mean (μ). The null hypothesis (H_0) in this case is that no sensors are erroneous, and thus the treatment effect (τ_i) is equal to zero for all s_i in A.

$$H_0: \tau_1 = \tau_2 = \tau_3 = \ldots = \tau_N = 0$$
$$H_1: \tau_i \neq 0 \text{ for at least one } i$$

Under the null hypothesis, each *Treatment* consists of μ with a random error component, with observations taken from the normal distribution of μ with overall variance (σ^2). In this case, the estimation error values of A' for each candidate sensor (s_i) are similar to one another. The hypothesis is tested by comparing two independent estimates of the population variance:

1. Variance between μ_i and μ: $(\mu_i-\mu)^2$
2. Variance within *Treatment*s: $(E_i-\mu_i)^2$

The first variance determines the difference between *Treatments* and the second variance determines the error within each *Treatment*. From the above two variances, we calculate sum of squares of *Treatments* variances:

$$SS_T = \sum_{i=1}^{N} (\mu_i - \mu)^2 \quad (11)$$

and sum of squares of error variance:

$$SS_E = \sum_{i=1}^{N} \sum_{j=1,\, j\neq i}^{N} (\mathbf{E}_{i,j} - \mu_i)^2 \quad (12)$$

By dividing SS_T and SS_E by their respective degrees of freedom (N-2 and ((N-1)N)-1), the mean square Treatment (MS_T) and mean square error (MS_E) are calculated. MS_E is an unbiased estimate of the σ^2 regardless of statistical difference between *Treatments*. On the other hand, MS_T is an unbiased estimate of the variance only if H_0 is true. The ratio $f_0=MS_T/MS_E$ has an *F*-distribution with degree of freedom N-2 and (N-1)N-1. Hypothesis H_0 is rejected if $f_0 > f_{\alpha,\, N-2,\, (N-1)N-1}$ [8]. Thus, using ANOVA, we test if a data set has erroneous sensors, at significance level α=0.05.

However, we do not know the location and number of erroneous sensors. To accomplish this task, we use Fisher's Least Significant difference (LSD). LSD compares all pairs of means with the t-statistic. The pairs of means are considered significantly different if

$$|\mu_i-\mu_j| > \text{LSD}$$

where,

$$\text{LSD} = t_{\alpha/2,(N-1)N-1}\sqrt{\frac{2MS_E}{n}} \quad (13)$$

An erroneous sensor will have mean that is significantly different from others ($p<0.05$). On the other hand, a "good" sensor will be statistically similar to all other non-erroneous sensors.

III. METHODS-EXPERIMENTAL

The proposed algorithmic framework is to be applied for detection of unreliable measurements and erroneous sensors in multi-sensor devices for biomedical instrumentation. The Biomedical systems of EIT and ECG are used as examples.

A. EIT Data

EIT data are acquired by successively applying a low amplitude low frequency current across each pair of electrodes while measuring the voltage differences produced on all the other pairs of electrodes. The measurement system used for these experiments has 16 electrodes. In adjacent current drive pattern, two adjacent electrodes are used for current injection and the remaining electrodes are used to make voltage measurements. Overall, there are N×(N-3) measurements available when all electrodes give good data. However, when there is one erroneous electrode, the total number of measurements available is reduced to (N-3)×(N-4). Typically, with sixteen electrodes the remaining "good" data are sufficient to reconstruct a reasonable image [2].

B. ECG Data

The system uses multiple surface electrodes to monitor the heart activity of a patient. Considering that these electrodes are monitoring the same medium, we would expect a relationship between the source (heart muscles) and sensors. A setup of the 12 lead ECG with 9 electrodes is used to acquire the data. There are 12 measurements: V_I, V_{II} and V_{III}, aV_R, aV_L, aV_F, V_1, V_2, V_3, V_4, V_5 and V_6. V_I, V_{II} and V_{III} and aV_R, aV_L, aV_F are based on measurements from Φ_L, Φ_R, and Φ_F. The remaining 6 measurements are from electrodes attached around the torso on the Transverse plane. V_2 and aV_F measure activity along the Sagittal plane. V_I, V_{II} and V_{III}, aV_R, aV_L, aV_F measure heart activity along Frontal plane[11]. This shows that the electrodes measure the heart activity along a specific plane and the measurements are inter-related to use the estimation scheme.

C. Simulated noise

The noise in EIT and ECG data is considered to be non-stationary since the mean and variance of the noise vary over time. However, the detection is performed over a time difference Δt which is generally treated stationary Gaussian. Therefore, simulated erroneous data is generated using representative non-erroneous data and additive Gaussian noise. The low level signal of the difference measurement is usually dominated by noise. Therefore, the signal power is measured and the additive noise data has relative magnitude for each data point. A simulated erroneous data is assumed to have one faulty sensor and Gaussian noise is added to data that is related to the faulty sensor.

IV. RESULTS

A. Electrical Impedance Tomography(EIT)

EIT Data were acquired from a previous study in which mechanically ventilated mongrel dogs were monitored with sixteen EIT electrodes spaced evenly around the shaved thorax [2, 13]. A representative set EIT data of ventilated dogs was used for data with no error (Figure 2A), and simulated erroneous data from electrode 5 was generated (Figure 2B). Applying the Fisher F-Test based decision parameter, we can look up the critical value at 95% with degree of freedom N-2 and (N-1)N-1. For this experiment the critical value corresponds to $f_{0.05,\,14,\,239}$=1.67. In Figure 2A the ratio f_0 is equal to 1.47, which is less than $f_{0.05,\,14,\,239}$=1.67; and H_0 cannot be reject at p<.05, and we conclude there are no erroneous electrodes. In Figure 2B, the electrode with errors has significantly lower T_i (p<0.05). The null hypothesis is rejected as the ratio f_0=2.71 is significantly higher than $f_{0.05,\,14,\,239}$.

To determine the sensitivity of the method, white Gaussian noise was added to the data of a particular electrode from a representative clean data. Data were calculated for SNR values from -50dB to 50dB, where simulations are repeated 100 times to calculate the error distribution. The resulting **F** ratio vs. SNR graph indicates the method can reliably detect an erroneous electrode when the SNR is below approximately 5dB (see Figure 3).

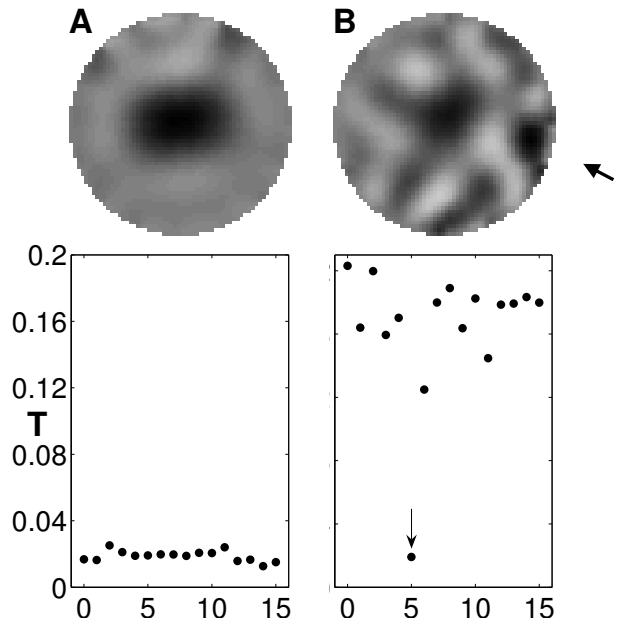

Figure 2: *Top:* (A) Reconstructed conductivity distribution of a dog thorax with no electrode error. (B) Reconstructed conductivity distribution of dog thorax with simulated erroneous electrode data of SNR=-10dB to electrode 5. Electrodes are numbered in the clockwise direction starting at 12 o'clock position. Dark colors are regions of low conductivity. *Bottom:* (A) *T* vs. electrode graph shows consistency in the absence of no erroneous electrode. (B) *T* vs. electrode graph shows *T* for electrode 5 is much lower than the rest of the *T* values, suggesting that electrode 5 is erroneous

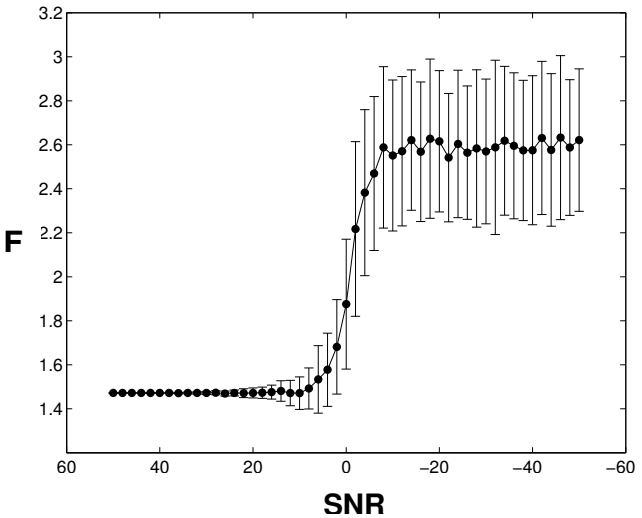

Figure 3: F statistic (± Std Dev) vs. SNR: Representative "good" data were used to analyze the sensitivity of the method. White Gaussian noise was added to electrode 5 (SNR: -50dB to 50dB). The experiment was repeated to determine the margin of error. The threshold for detection is at a SNR of 5dB.

B. Electrocardiogram (ECG)

The ECG data were from the online database of [11]. We categorize the data into two classes: non-erroneous and erroneous data due to synthetic noise. The first data category is used to establish how well the scheme can estimate data based on the forward and inverse model. The second data category is used to observe the sensitivity of the data to noise.

Before applying our sensor error detection scheme for ECG, we need to establish the number of independent sources that contribute to the ECG signal and determine its dimensionality. One way to establish dimensionality is by decomposing the data into its eigenvector and eigenvalue. The most dominant vectors are represented with large eigenvalues. The eigenvalue analysis shows that the maximum number of sources present for an ECG data is seven. As confirmation, [12] showed that ECG is generated due to electrical activity of seven different tissues of the heart that make up the typical QRS amplitude. Hence, the QRS amplitude is the linear sum of the action potential of the seven sources. The seven signals are generated in different times by different tissues and do not contribute information regarding other sources which makes them statistical independent. It is also clear to see that the signals are non-Gaussian.

A 12-Lead system measures activity over three measurement planes: V_2 and aV_F measure activity over the Sagittal plane (X-Z plane), aV_R, aV_L, I, II, aV_F and III measure activity over the Frontal plane (Z-Y plane), and V_1 to V_6 measure activity over the Transverse plane (X-Y plane). The possibility of estimating the measurement of a specific electrode from the other electrodes becomes difficult as only a fraction of the 12 leads are observing the data from the similar plane. Moreover, the data for Sagittal plane and Frontal plane is constructed out of 6 Leads determined from 3 electrodes (measurement points) [12]. Any two Leads contain exactly the same information as the remaining four. Therefore, this characteristic violates the assumption that the data from each lead is an independent measure of ECG signal used to estimate error from a single electrode. In addition, the three measurement points are situated further away from the heart (limb, shoulder and ankle) making ECG signal weaker and susceptible to noise from EEG signal and other sources. For the above reasons the estimation scheme was only applied to electrodes along the Transverse plane on the chest. Figure 4, shows the original data from electrode 4 and its estimate based on the transverse plane. This figure demonstrates that data from the Transverse plane, based on **H** and **R**, created through SVD is sufficient as an estimate.

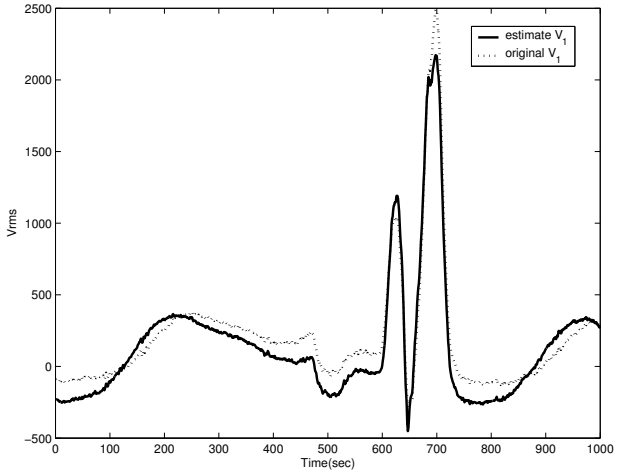

Figure 4: Original data (dotted line) and estimate (solid line) of original data: **H** and **R** estimated based on data of the transverse plane. The data is from electrode 4 (V_1)

Synthetic erroneous ECG data is generated by adding white Gaussian noise to a specific sensor data. This data is used to validate the detection scheme introduced in the previous section. Figure 5 shows an ECG data corrupted with White Gaussian noise of 0 dB SNR on data from electrode 4. When the detection scheme is applied, it is clear to see that the estimation error of all electrodes except electrode 4 is high. The corrupted data from electrode 4 is contributing to a model that cannot properly estimate the other electrodes. However, the f-value for the ECG data with no erroneous electrode is greater than $f_{\alpha, N-2, (N-1)N-1}$

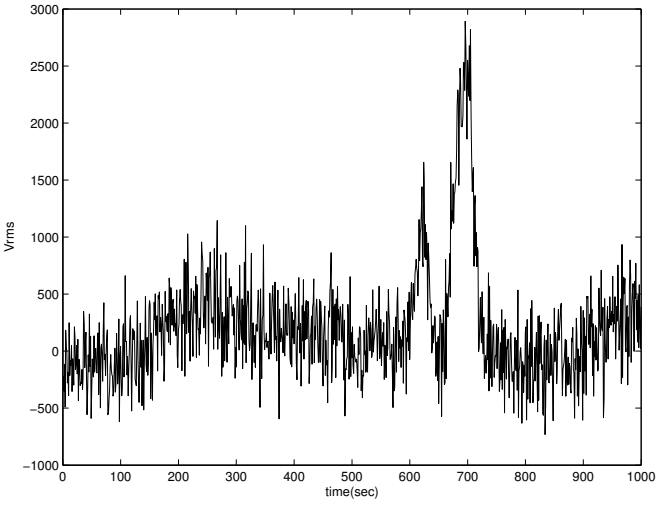

Figure 5: (a) Corrupted ECG data from electrode 4 with 0dB noise

The detection threshold of the method on Transverse plane is determined by adding White Gaussian noise from -50 to 50 dB and plotting the F statistics vs. SNR. Looking at the resulting graph in Figure 6, we can clearly see a jump in the f-value after 0dB of SNR. The null hypothesis is rejected if the f-value is less than $f_{0.01,4,29} = 4.12$. Based on the above critical f-value, we can conclude that the system is sensitive to noise levels of 0dB for data on the transverse plane.

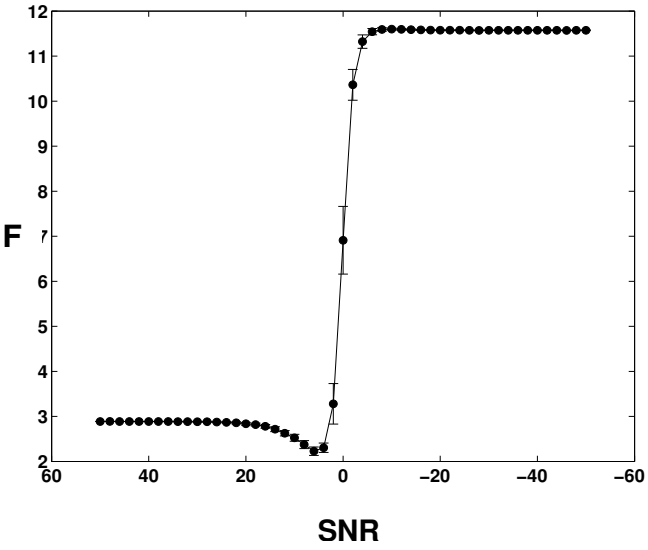

Figure 6: F vs. SNR: F statistic (± Std Dev) vs. SNR: Representative "good" data were used to analyze the sensitivity of the method. White Gaussian noise was added to electrode 4 (SNR: -50dB to 50dB). The experiment was repeated to determine the margin of error. The threshold for detection is at a SNR of 0dB.

V. CONCLUSION

In this paper, we have presented a method to automatically detect erroneous sensors in multi-sensor system, such as EIT and ECG. The method is based on the model that an erroneous sensor produces measurements inconsistent with those from other good sensors. Multi-sensor systems were divided into two categories: known and unknown system models. A known system model has an underlying relationship between the measurement and the medium that is independent of the data. Whereas an unknown system model, does not have an obvious underlying relationship and can only be deduced based on the available data.

Based on these two system model definitions, an estimation scheme was developed to handle both scenarios. Results show that the method is able to correctly detect the presence of noise and identify the location of erroneous sensors in representative EIT and ECG data. The decision criterion is based on ANOVA and shows that detection of one or more erroneous sensor is feasible above a specific SNR level. White Gaussian noise was added to a specific electrode, as in Figure 2 and 5, and the algorithm was tested based on the appropriate estimation scheme.

The analysis showed erroneous electrode in EIT can be detected at noise level of 5dB with $p<0.05$, see Figure 3. The result for ECG based on data from the transverse plane showed that detection of erroneous electrodes is possible above 0dB with $p<0.01$, see Figure 6. Our attempt to incorporate data from all 12-Leads failed due to lack of data independence as 6 of the Leads are determined from 3 electrodes only. Moreover, the fact that several of the Leads acquired the data from different planes complicated the modeling. Nevertheless, the data acquired from the 6 electrodes measuring ECG signal on the transverse plane was successfully used demonstrate the algorithm.

Automatic detection of sensor errors in multi-sensor system has several possible applications. In offline processing, such a technique could identify and correct for such errors. More usefully, if implemented in multi-sensor monitoring equipment, it would be possible to alert staff who could then attend to the problem. However, for such online applications, the algorithm is still slow (5s) for real-time data analysis, but would permit erroneous sensor detection in the background.

REFERENCE

[1] A Adler and R Guardo, "Electrical Impedance Tomography: Regularised imaging and Contrast Detection", *IEEE Trans. Medical Imag*. Vol. 15, No. 2, pp. 170-179, April 1996

[2] A Adler, R Amyot, R Guardo, J H T Bates, Y Berthiaume, "Monitoring changes in lung air and liquid volumes with electrical impedance tomography", *J. Appl. Physiol.,* Vol. 83, No. 5, pp. 1762-1767, Nov 1997

[3] Y Asfaw and A Adler, "Automatic detection of erroneous electrodes in Electrical Impedance Tomography", *Physiol. Meas.*, In press

[4] F Al-Hatib, "Patient-instrument connection errors in bioelectrical impedance measurement", *Physiol. Meas*., Vol. 19, No. 2, pp. 285-296, May 1998

[5] A Lozano, J Rosell and R Pallás-Areny, "Errors in prolonged electrical impedance measurements due to electrode repositioning and postural changes", *Physiol. Meas.,* Vol. 16, No. 2, pp. 121-130, May 1995

[6] S Meeson, B Blott, and A Killingback, "EIT data noise evaluation in the clinical environment", *Physiol. Meas.,* Vol. 17(suppl.), No. 4A, pp. A33-A38, November 1996

[7] R Aster, B Borchers, and C Thurber, "Parameter Estimation and Inverse Problems", *Academic Press*, 2004

[8] DC Montgomery and GC Runger, "Applied Statistics and Probability for Engineers Chapter 13: Design and analysis of single factor experiments: The analysis of variance", 3rd ed, John Wiley & sons inc, 2002

[9] CJ James and CW Hesse, "Independent component analysis for biomedical signals", *Physiol. Meas.,* Vol. 26 , No. 1, pp. R15-R39, February 2005

[10] Shlens J., "A Tutorial on Principal Component Analysis", http://www.snl.salk.edu/~shlens/pub/notes/pca.pdf , December 2005

[11] M Oeff, "The PTB Diagnostic ECG Database", http://www.physionet.org/physiobank/database/ptbdb/

[12] JG Webster, "Medical Instrumentation", John Wiley & Sons, 3rd ed, 1998

[13] Guardo, R., Boulay, C., Murray, B., and Bertrand, M., "An experimental study in electrical impedance tomography using backprojection reconstruction", IEEE Trans. on Biomedical Engineering. Vol. 38, Issue 7, pp. 617-627, July 1991.

[14] Haigh K., and Yanco H., "Automation as Caregiver: A survey Of Issues and Technologies", AAAI Technical Report WS-02-02, pp. 39-53, 2002

[15] Bai J., Zhang Y., Shen D., Wen L., Ding C., Cui Z., Tian F., Yu B., Dai B., Zhang J., "A portable ECG and blood pressure telemonitoring system",IEEE Eng. In Medicine and Biology Magazine, Vol. 18, Issue 4, pp. 63-70, July 1999

[16] Malmivuo J. and Plonsey R., "Bioelectromagnetism: Principles and Applications of Bioelectric and Biomagnetic Fields",Oxford University Press, 1995